Chemistry and Physics of Lipids 218 (2019) 57–64

Contents lists available at ScienceDirect

Chemistry and Physics of Lipids

journal homepage: www.elsevier.com/locate/chemphyslip

Physical states and thermodynamic properties of model gram-negative bacterial inner membranes

Javier Hoyo, Juan Torrent-Burgués, Tzanko Tzanov*

Grup de Biotecnologia Molecular i Industrial, Department of Chemical Engineering, Universitat Politècnica de Catalunya, Rambla Sant Nebridi 22, 08222, Terrasa, Spain

ARTICLE INFO

Keywords:
Phosphatidylethanolamine
Phosphatidylglycerol
Cardiolipin
Lipid-lipid interactions
Bacterial mimetic membranes
Escherichia coli

ABSTRACT

Novel antimicrobial agents are focused to interact with the bacterial membrane whose lipid composition (number and position of unsaturations and lipid headgroup) is adapted according to environmental signals. The anticipation of the adapted membrane properties is of high relevance to increase the targetability of such drugs. Herein, natural lipids extracted from *Escherichia coli* -phosphatidylethanolamine (PE), phosphatidylglycerol (PG) and cardiolipin (CL)- are used to form biomimetic membranes constituted by several PE:lipid ratios using the Langmuir and Langmuir-Blodgett techniques. The use of these techniques and the natural myriad of each lipid structures that constitute the biological *E.coli* membrane establishes a simple and reproducible model to evaluate the lipid-lipid interactions. PE and PG present similar shape and size, thus establish ideal and fluid -liquid expanded (LE) state - mixtures, whereas the differences between PE and CL motivate the formation of non-ideal and fluid (LE state) mixtures. The same physical state and the minor differences in elasticity (differences in the inverse of the compressibility modulus $< 15\,mN{\cdot}m^{-1}$) between both systems regardless the PE content in the (PE:lipid) mixture suggest that the changes in the lipid composition influence the membrane proteins function rather than affecting the rigidity of the bacterial membrane.

1. Introduction

The appearance of bacterial strains with resistance to conventional antibiotics is a major global healthcare problem prompting research on novel therapeutic approaches. (Ivanova et al., 2017) Currently, different strategies are followed to eradicate bacteria, involving most of them the disruption of the bacterial membrane structure (Ferreres et al., 2018; Salat et al., 2018) causing osmotic damage and flow of cytoplasmic components out of the cell causing the cell death. Bacteria regulate their membrane lipid composition and the degree of unsaturation of their hydrocarbon chains as a response to environmental signals (Larsson and Törnkvist, 1996; Shokri and Larsson, 2004). For instance, *Escherichia coli (E.coli)* balances the quantity of phosphatidylglycerol (PG) in detriment of cardiolipin (CL) according to the growth rate and increases the content of CL to save energy and carbon, (Shokri and Larsson, 2004) and *Pseudomonas aeruginosa* increases the length of the lipid chains when changing from planktonic to sessile form resulting in a decrease of the membrane fluidity. (Benamara et al., 2011) These changes affect the activities of membrane proteins by influencing the chemical and physical membrane properties or affecting the annular lipids in direct contact with integral membrane proteins (Lee, 2004). Therefore, a deeper knowledge of the physical states and elasticity of these lipid membranes is necessary to anticipate their targeting and destabilization by any novel antimicrobial agent.

Gram-negative bacteria such as *E.coli* have an outer membrane – mainly composed of lipopolysaccharides - and a cytoplasmic membrane which is composed by proteins and the following phospholipids (Scheme 1): ~ 77% phosphatidylethanolamine (PE), ~ 13% PG, and ~ 10% CL. (Shokri and Larsson, 2004; Yeagle, 2016) PE is a zwitterionic phospholipid with a headgroup formed by a phosphate (negative charge) and a free amine (positive charge). Two hydrophobic acyl chains constitute its tail. (Lee, 2003) PE is the most abundant phospholipid in bacterial membranes and the second most abundant in mammalian (~ 20%), (Vance, 2015) plants and yeast membranes. PE is essential for *E.coli* growth, and in addition to be the membrane main constituent, interacts with several membrane proteins such as lactose

Abbreviations: AFM, atomic force microscopy; CL, cardiolipin from *E. coli*; CLP, cardiolipin from bovine heart; DPPE, dipalmitoylphosphatidylethanolamine; DPPG, dipalmitoylphosphatidylglycerol; *E.coli*, *Escherichia coli*; PLE, *E. coli* polar lipid extract; LB, Langmuir-Blodgett; LC, liquid condensed; LE, liquid expanded; POPE, palmitoyloleoylphosphatidylethanolamine; POPG, palmitoyloleoylphosphatidylglycerol; PE, phosphatidylethanolamine from *E. coli*; PG, phosphatidylglycerol from *E. coli*; SPB, supported planar bilayers

* Corresponding author.
E-mail address: tzanko.tzanov@upc.edu (T. Tzanov).

https://doi.org/10.1016/j.chemphyslip.2018.12.003
Received 11 October 2018; Received in revised form 16 November 2018; Accepted 5 December 2018
Available online 06 December 2018
0009-3084/

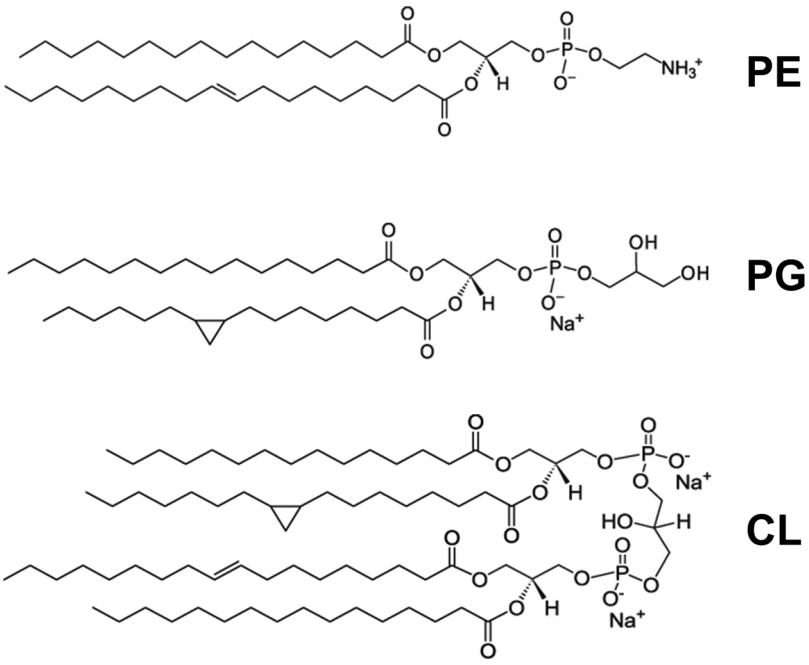

Scheme 1. Representative chemical structure of the myriad of lipid structures that shares the same headgroup: phosphatidylethanolamine (PE), phosphatidylglycerol (PG) and cardiolipin (CL) in lipid extracts from *E. coli* (see Section 2.1).

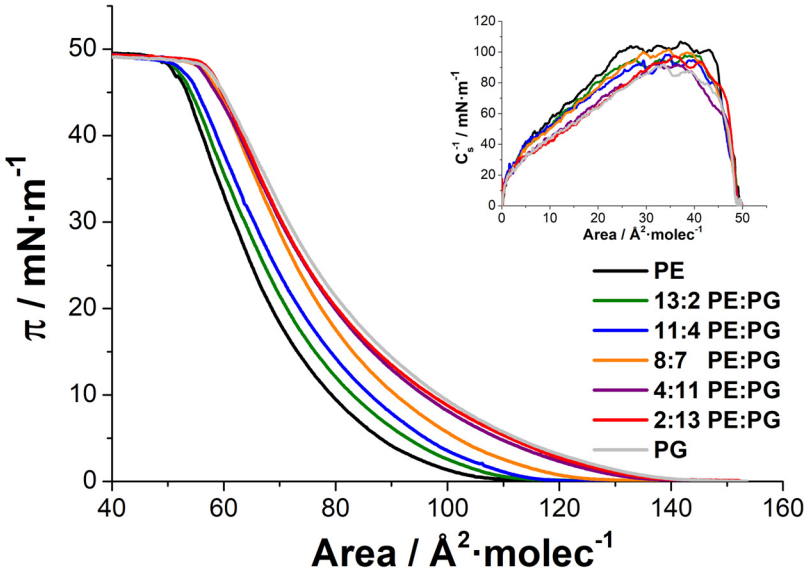

Fig. 1. π-A isotherms for PE, PG and PE:PG mixtures on PBS subphase. Inset: Inverse of the compressibility modulus vs. surface pressure corresponding to the described π-A isotherms.

permease. (Dowhan and Bogdanov, 2012) PG is an anionic phospholipid that contains two acyl chains esterified to glycerol and a phosphate headgroup (Yeagle, 2016). The diphosphatidylglycerol lipid (CL) presents a dimeric structure with two negative phosphate charges on its small headgroup and a large hydrophobic part built from four acyl chains (Schlame et al., 2000; Khalifat et al., 2011) and is mainly found in the inner mitochondrial membrane (10–15%) (Horvath and Daum, 2013). PG and CL are scarcely found in mammalian cell membranes (< 5%) (Vance, 2015) and are involved in the binding of transmembrane proteins. (Yeagle, 2016)

Biomimetic membranes have been designed to mimic biological membranes, based on supported planar bilayers (SPB) and Langmuir monolayer films. (Hoyo et al., 2012; Castellana and Cremer, 2006) The high reproducibility and versatility of Langmuir films make them a convenient model system to investigate the properties of such membrane models. (Hoyo et al., 2015a, b) The Langmuir and Langmuir-Blodgett (LB) film techniques have been applied to elucidate the interactions between major thylakoid membrane lipids (Hoyo et al., 2016), lipid-polymer interactions (Purrucker et al., 2004; Kowal et al., 2015), lipid-peptide interactions (Dennison et al., 2014, 2009) and the interplay between redox molecules and lipid biomimetic membranes (Hoyo et al., 2015a, 2013). Model bacterial inner membranes obtained by these techniques have been successfully applied in our group to study the interaction of sonochemically generated antibiotic (Fernandes et al., 2017) and layer-by-layer coated nanoparticles (Ivanova et al., 2018).

In the current work, the Langmuir and LB techniques are used to study the physical states and thermodynamic properties of PE:PG and

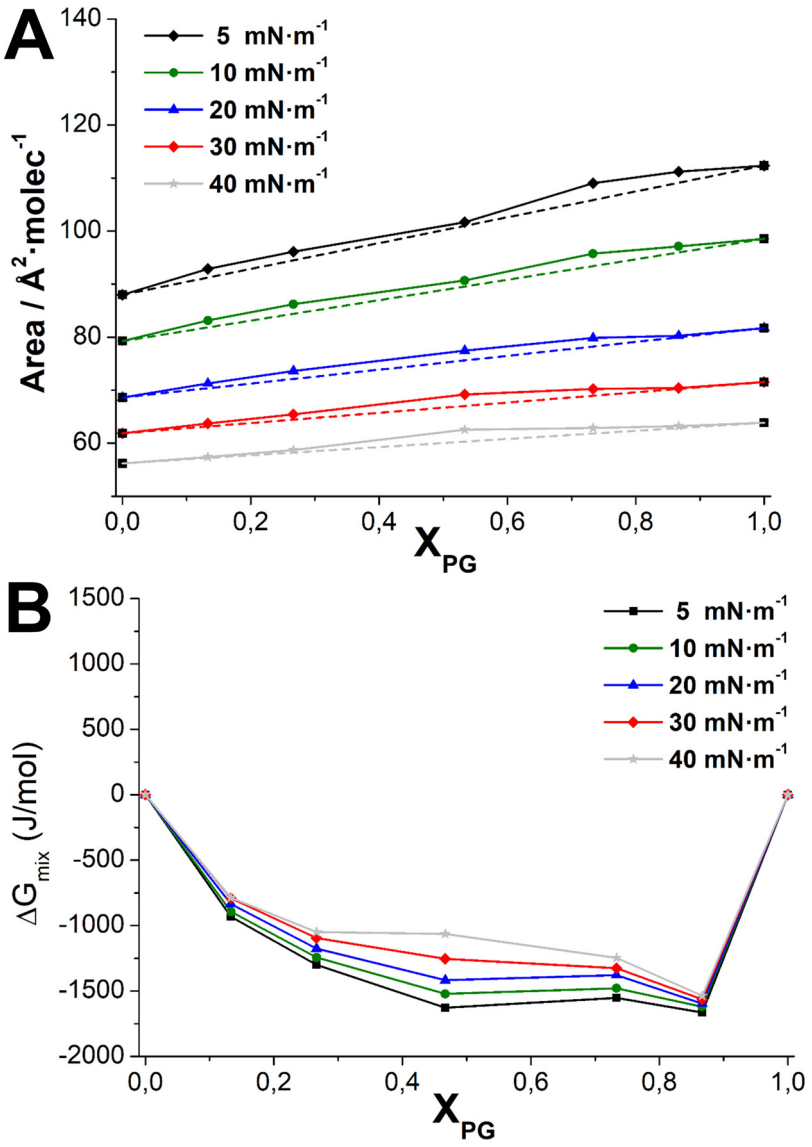

Fig. 2. A) Mean area per molecule vs. molar fraction and B) mixing energy vs. the molar fraction at several surface pressures for the PE:PG system. Discontinuous straight line represents the ideal behaviour for each surface pressure.

PE:CL monolayers at the air/water interface by using natural lipid extracts from *E. coli*. LB films of these systems transferred to mica sheets are used to characterize their topography. The range of interactions that may occur in natural bacterial inner membranes as a response to external stimuli are of major relevance for the design of new antibacterials.

2. Materials and methods

2.1. Materials

The lipids used herein -Avanti Polar Lipids, Inc. (Alabama, USA)- are extracted from *E. coli* and are designed as PE, PG and CL to englobe all the present structures containing the same headgroup. The precise composition of the myriad corresponding to each headgroup can be found at www.avantilipids.com PE (♯ 840027), PG (♯ 841188) and CL (♯ 841199). All other reagents were obtained from Sigma-Aldrich (Spain) and used without further purification. Ultrapure MilliQ water with a resistivity of 18.2 MΩ · cm^{-1} was used in cleaning procedures and for phosphate buffer solution (PBS) at pH 7.4 preparation. Mica sheets were purchased from TED PELLA Inc (CA).

2.2. Langmuir and Langmuir-Blodgett films

Stock solutions of PE, PG, and CL were prepared by dissolving the corresponding lipid in chloroform. Afterward, the appropriate amount of each stock solution was mixed to obtain the corresponding lipid mixture, named in molar ratio. The lipid solutions were used within 15 days and kept at - 20 °C.

The bacterial inner membrane model was assessed using Langmuir monolayer films of the PE:PG and PE:CL systems in PBS subphase; using a Langmuir trough equipped with two mobile barriers (KSV NIMA Langmuir-Blodgett Deposition Troughs, model KN2002, Finland) with a total area of 273 cm^2 and total volume 120 cm^3 mounted on an anti-vibration table and housed in an insulation box at a temperature of 23 ± 1 °C. The surface pressure (π) was measured by a Wilhelmy balance and registered during the course of the π – Area (A) isotherm. All π – A isotherms and LB films were performed by triplicate for reproducibility control.

2.3. Langmuir monolayer compression measurements

The Langmuir trough was cleaned with chloroform, water and by

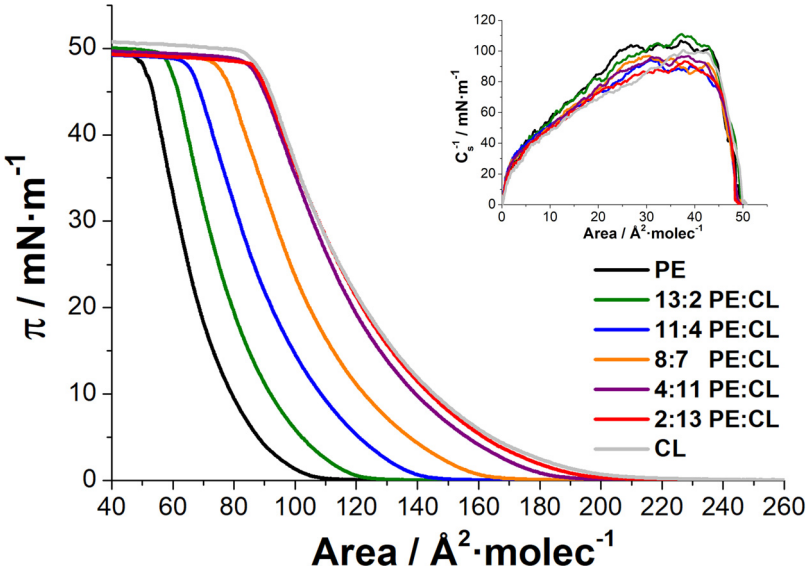

Fig. 3. π-A isotherms for PE, CL and PE:CL mixtures on PBS subphase. Inset: Inverse of the compressibility modulus vs. surface pressure corresponding to the described π-A isotherms.

surface suctioning until the baseline of the subphase (PBS) ensured cleanliness. Afterward, 25 μL (0.5 mg mL^{-1}) of the lipid or lipid mixture solution are dropwise added into the trough by the use of a gas-tight syringe. The barrier closing speed was set at 25 cm^2 min^{-1} and the recording of the π – A isotherm started after lagging 10 min for complete evaporation of chloroform and homogeneous spread of the lipids on the trough surface area.

2.4. Langmuir-Blodgett monolayer transfer

LB monolayers of the single lipid constituents and the 11:4 PE:PG and 11:4 PE:CL mixtures, corresponding to the average biological composition of *E. coli* membranes[8] were transferred to mica surface at π = 3 and 33 mN·m^{-1}. Firstly, freshly cleaved mica was dipped through the air/liquid interface on the subphase before adding the lipid solution. Afterward, the barriers compressed until the setpoint was achieved and 20 min were lagged prior rising the mica at 1 mm·min^{-1} linear velocity.

2.5. Topography characterization

Atomic force microscopy (AFM) topographic images of LB films transferred to mica were acquired in an air tapping mode using a Multimode AFM controlled by Nanoscope IV electronics (Veeco, Santa Barbara, CA) under ambient conditions. Triangular AFM probes with silicon nitride cantilevers and silicon tips were used (SNL-10, Bruker) with a nominal spring constant of 0.35 N·m^{-1} and a resonant frequency of 50 kHz. Images were acquired at 1 Hz line frequency and at minimum vertical force to reduce sample damage.

2.6. Data analysis

2.6.1. Physical states

The inverse of the compressibility modulus (C_s^{-1}) provides information about the elasticity and the compressibility of the corresponding monolayer and is used for physical state identification. C_s^{-1} is obtained from the π-A isotherms calculated according to Eq. (1), where A is the mean area per molecule (Å^2·molecule^{-1}), π the surface pressure (mN·m^{-1}) and T the absolute temperature (K).

$$C_s^{-1} = -A\left(\frac{d\pi}{dA}\right)_T \quad (1)$$

2.6.2. Thermodynamic study

The stability of the mixture is correlated to its mixing energy (ΔG_{mix}) and is obtained from the following equation in which A^E represents the excess area, A_1 and A_2 the area per molecule for the individual components, A_{12} the mean area per molecule for the mixture, x_1 and x_2 the molar fraction for each component, G^E the excess free energy of mixing, N_A the Avogadro's number, R the gas constant and T the absolute temperature.

$$A^E = A_{12} - (X_1A_1 + X_2A_2) \quad (2)$$

$$G^E = N_A \int_0^{\pi} A^E \, d\pi \quad (3)$$

$$\Delta G_{mix} = \Delta G_{id} + G^E \quad (4)$$

$$AG_{id} = RT\,(x_1 \ln x_1 + x_2 \ln x_2) \quad (5)$$

3. Results and discussion

3.1. π-A isotherms, physical states and mixing behaviour

PE and PG showed the lift-off area at 110 and 140 Å^2·molecule^{-1} respectively, and both presented a monotonic increase until the collapse region, at π = 49 mN·m^{-1} (Fig. 1). The C_s^{-1} curves show the maximum ($C_s^{-1}{}_{max}$) at ≈ 105 and 90 mN·m^{-1} for PE and PG respectively. These observations indicate that both phospholipids are in liquid-expanded (LE) physical state until the collapse of the monolayer. (Vitovič et al., 2006) Similar isotherms and C_s^{-1} curves in terms of shape, collapse pressure and physical state were observed for the PE:PG mixtures and the corresponding pure phospholipids. This similar performance was anticipated based on the close size and shape of both phospholipids, in particular of their hydrocarbon tails. The differences observed are correlated with the slightly higher PG headgroup size than that of PE, thus affecting the lift-off area which increased with the PG content in the PE:PG mixture.

The mean area per molecule vs the PG molar fraction curves (Fig. 2A) showed a monotonic increase from pure PE to pure PG and exhibited practically negligible deviation from the ideal behaviour (dashed line), indicating that both phospholipids form ideal monolayers at the air/water interface. Negative values of the ΔG_{mix} curves (Fig. 2B) were obtained for all the mixtures and surface pressures. Moreover,

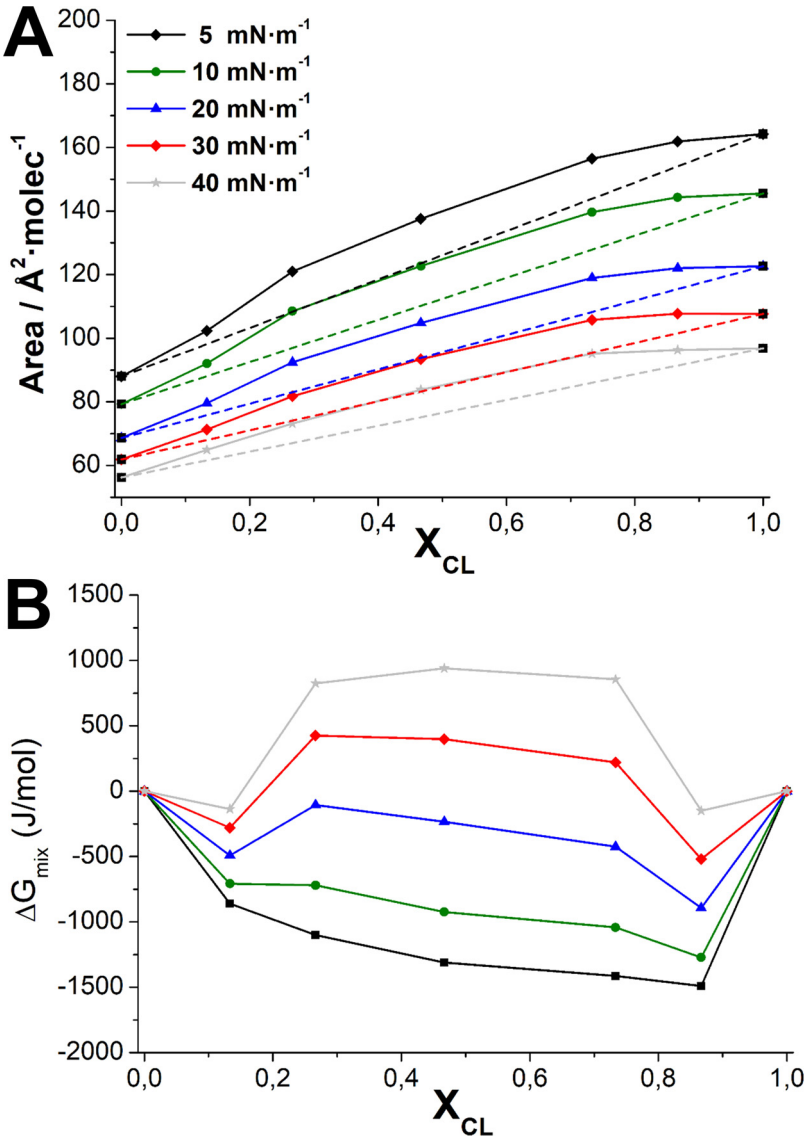

Fig. 4. A) Mean area per molecule vs. molar fraction and B) mixing energy vs. the molar fraction at several surface pressures for the PE:CL system. Discontinuous straight line represents the ideal behaviour for each surface pressure.

minor increase of ΔG_{mix} is observed upon scaling the surface pressure indicating that PE and PG are ideally mixed and form stable monolayers. (Roche et al., 2006) As explained above, the similar shape and size of both phospholipids favour the formation of ideal mixtures. These results are in agreement with the molecular dynamics simulation of a hydrated mixed palmitoyloleoylphosphatidylethanolamine (POPE) and palmitoyloleoylphosphatidylglycerol (POPG) membrane in a molecular ratio similar to the biological one, which showed water bridging, direct H-bonding and ion bridging between POPE and POPG. (Murzyn et al., 2005) The authors claimed that POPE interacts primary with POPG molecules and secondary with other POPE molecules whereas POPG rarely interacts with other POPG molecules (Murzyn et al., 2005). In this line, phosphatidylethanolamine and phosphatidylglycerol phospholipids with their hydrocarbon chains fully saturated (dipalmitoylphosphatidylethanolamine (DPPE) and dipalmitoylphosphatidylglycerol (DPPG)) showed also DPPE-DPPG associates between molecules being favored by the similar shape and size coupled to the absence of unsaturations (Wydro et al., 2012).

The CL π-A isotherm (Fig. 3) presented a regular increase until the collapse of the monolayer at $\pi = 49\,mN{\cdot}m^{-1}$, the lift-off area at $220\,Å^2{\cdot}molecule^{-1}$ and the $C_s^{-1}{}_{max} \approx 98\,mN{\cdot}m^{-1}$ (inset of Fig. 3), confirming[28] the LE physical state of CL film. Oppositely, Langmuir films of cardiolipin from bovine heart (CLP) at $30\,mN{\cdot}m^{-1}$ formed LC state, (Chen et al., 2011) which is attributed to the differences in the unsaturations number and position between CL and CLP.

The PE:CL mixtures and the corresponding pure phospholipids show high similarities both in isotherms and C_s^{-1} curves: shape, collapse pressure and physical state. The similar length and unsaturation degree of the hydrocarbon tails of both phospholipids explains these observations. However, the lift-off area fairly increases as the CL content in the PE:CL mixture is scaled. CL bears four hydrocarbon chains linked to the headgroup, unlike the two chains of PE, which induces a larger base of the conical shape of the CL molecule compared to PE. (Baumgärtner et al., 2007; Boyd et al., 2017).

The mean area per molecule vs. molar fraction curves (Fig. 4A) showed an increase from pure PE to pure CL and exhibited positive deviations from the ideal behaviour (dashed line) indicating that both phospholipids form non-ideal monolayers at the air/water interface. The negative values of the ΔG_{mix} curves (Fig. 4B) at low surface pressures indicated the stability of the lipid mixture monolayer. Nevertheless, positive values were observed for most of the mixtures upon increasing the surface pressure, although their magnitude is small. In

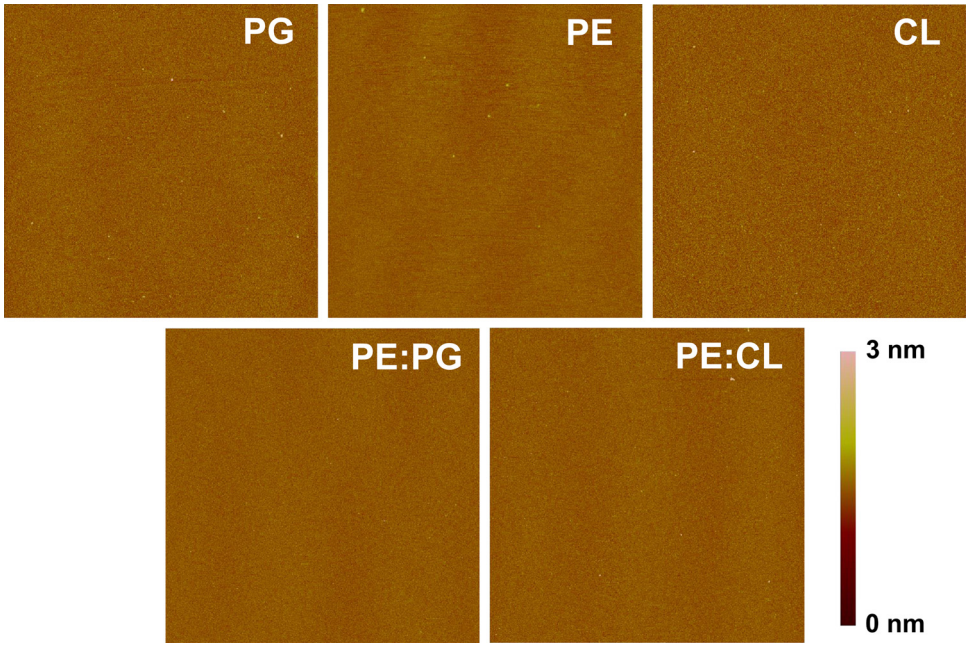

Fig. 5. AFM images (5 × 5 μm) of LB monolayers of the single lipid constituents (PE, PG, CL), 11:4 PE:PG mixture and 11:4 PE:CL mixture transferred to mica at $\pi = 3\,mN{\cdot}m^{-1}$.

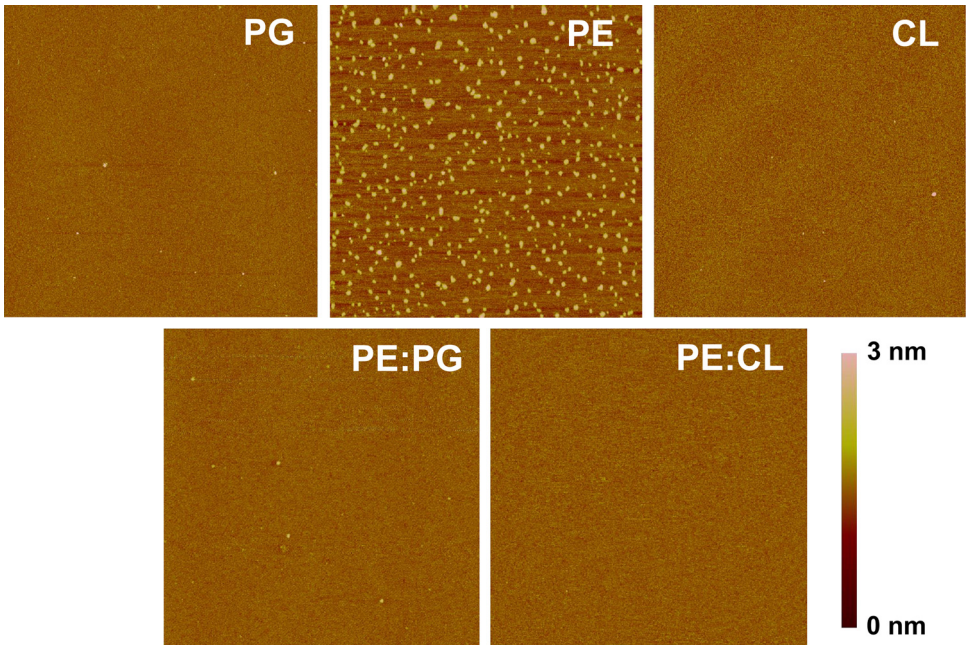

Fig. 6. Topographic AFM images (5 × 5 μm) of LB monolayers of the single lipid constituents (PE, PG, CL), 11:4 PE:PG mixture and 11:4 PE:CL mixture transferred to mica at $\pi = 33\,mN{\cdot}m^{-1}$.

addition, the ΔG_{mix} corresponding to each mixture increased scaling the surface pressure, and changed from negative to positive values. Therefore, PE and CL are non-favoured mixtures (20–80 % of CL) at surface pressure close to that of real biological membranes ($\approx 33\,mN{\cdot}m^{-1}$) (Cevc and Marsh, 1987) suggesting the possibility of lateral phase separation (Sanchez and Badia, 2003).

The net repulsive interactions predominate in the films that is correlated to the shorter intermolecular distances associated with high surface pressures and the structural differences of the phospholipids. (Bottier et al., 2007) Previous atomic-scale molecular dynamics simulations confirmed our empirical observations revealing no influence of CL in membrane condensation or hydrocarbon chain order in PE bilayers, where the PE-PE hydrogen bonds are more stable and frequent than the PE:CL ones (Róg et al., 2009). On the other hand, multilamellar vesicles and LB monolayers constituted by DPPE and CLP showed the presence of lipid domains (Lupi et al., 2008) and SPB formed with mixtures containing POPE and CLP showed also the formation of such domains (Domènech et al., 2007). In both cases, the differences in the number and position of the unsaturations in the hydrocarbon chain facilitated the lateral phase separation. AFM topographic images were performed (Section 3.2) to elucidate the presence of lateral phase separation in the current systems, in particular the corresponding to the average biological PE:lipid ratio 11:4.

3.2. Topography characterization

AFM images of LB films on mica of single lipid constituents PE, PG and CL, and the selected mixtures were studied at the very fluid physical state ($\pi = 3\ mN{\cdot}m^{-1}$), see Fig. 5, and at the internal lateral surface pressure ($\pi = 33\ mN{\cdot}m^{-1}$), (Cevc and Marsh, 1987) see Fig. 6, of natural cell membranes. Most of the images showed mainly one shade that indicated the presence of only one physical state corresponding to LE phase, as was observed in the insets of Figs. 2 and 4. PE at $\pi = 33\ mN{\cdot}m^{-1}$ presents two shades (light and dark) that are related to the LE phase (dark shade) and liquid condensed (LC) phase (light shade). Such assignment was based on the different tilting of the phospholipid molecules for each physical state. The presence of LC phase is not strictly anticipated in the inset of Fig. 2, but the proximity of the observed $C_s^{-1}{}_{max}$ value to the lower limit for the LC formation (Vitovič et al., 2006) and the mica-lipid interaction suggested the formation of ordered domains (LC phase) once the surface pressure achieved that of the natural cell membranes. On the other hand, the AFM images of the PE:PG and PE:CL mixtures show absence of lateral phase separation both at $\pi = 3$ and $33\ mN{\cdot}m^{-1}$ in spite of the thermodynamic results for the PE:CL system at $\pi \geq 30\ mN{\cdot}m^{-1}$ (Fig. 4B) that pointed the possibility of phase segregation. The no observation of such domains may be related to the LE state of the films that mask their presence, as will be discussed later.

3.3. The role of the lipid composition in real bacterial inner membranes

In a basic model membrane, biological membranes are composed of membrane lipids and membrane proteins, thus establishing lipid-lipid, protein-protein and lipid-protein interactions, which in turn, are dependent on each other. (Yeagle, 2014) In the current article, we studied the lipid-lipid interactions through monolayers films formed both at the air/liquid (Figs. 1–4) and air/mica (Figs. 5 and 6) interface as models of bacterial inner membranes. Guidalevitz et al. (Gidalevitz et al., 2003) and Clausell et al. (Clausell et al., 2007) engineered a simple model for mimicking both layers of the bacterial membrane. The outer layer was made of lipopolysaccharide (LPS) whereas the inner one was DPPG or POPG. The absence of the zwitterionic lipid (PE) that counts for the ≈ 77% of the total lipid content of the inner membrane (Yeagle, 2016) reduced the reliability of the system. Recently, Michel et al. (Michel et al., 2015; Michel et al., 2017) mimicked the outer and inner leaflets by the use of, respectively, LPS and a ternary mixture of phospholipids containing monounsaturated lipids with the headgroups PE, PG and CL. Even these works studied a more realistic membrane model; they lack on the use of the different lipid structures that constitute the bacterial membrane and share the same headgroup, thus reducing the elasticity of the biomimetic membranes and consequently, the reliability of the model. López-Montero et al. (López-Montero et al., 2010, 2008) prepared more reliable inner bacterial membranes by using the *E. coli* polar lipid extract (PLE) that is constituted by the lipid structures that shares the same headgroup. In line with the model of Lopez-Montero et al., we have used the myriad of each lipid structures that constitute the biological *E.coli* membrane rendering a fluid membrane that correlates with the natural (de Mendoza and Cronan, 1983) one and establishes similar lipid-lipid interactions. Additionally, the current work presents two binary lipid systems comprising one zwitterionic and one anionic lipid and studies different lipid ratios, including the biologically relevant one, thus the lipid-lipid interactions observed in our binary system can anticipate those occurring in the natural ternary one. The use of several ratios permit the evaluation of the lipid-lipid interactions mimicking the bacterial membrane adapted to external stimuli. Even at non-biological ratios, the biomimetic membranes show similar rigidity indicating that within biological ratios the rigidity of the inner membrane is very little changed upon bacterial adaptation to the environment.

PE and PG lipids with their hydrocarbon chains fully saturated show an almost cylindrical shape. However, the bacterial PE and PG contain unsaturations that wide the base of the cylinder, thus achieving a conical shape. (Baumgärtner et al., 2007) The intrinsically conical shape of CL lipid molecule with saturated acyl chains wides the base of the cone upon increasing the number of unsaturations. The cone shape motivates steric hindrances in the lipid packing upon compression of the monolayer due to the reduction of the van der Waals and hydrogen bonding forces, thus preventing the lipid mixture monolayer from achieving the ordered LC state (Figs. 1, 3 and 6). (Hoyo et al., 2016;Popova and Hincha, 2003) The base of the cone of PE and PG molecules, comparably smaller than the one of CL, and the similar size of both lipids caused stable and ideal monolayers (Fig. 2). On the other hand, the PE and CL difference in size yielded non-ideal mixtures with tendency to phase separation and formation of enriched domains (Sanchez and Badia, 2003) at a surface pressure close to that of bacterial membranes. The formation of enriched domains, however, is not observed in AFM images of the PE:CL films at $\pi = 33\ mN{\cdot}m^{-1}$ (Fig. 6) most probably due to the high elasticity of the mixture film (LE state). Our images agree well with the AFM observations of Mitchel et al. (Michel et al., 2015, 2017) for a lipid system that contained PE, PG and CL headgroups with monounsaturated chains that also established elastic films. Lopez-Montero et al. (López-Montero et al., 2010, 2008) however did observe the presence of lipid domains by Brewster angle microscopy and fluorescence microscopy for the single ternary mixture PLE, which presented comparable elasticity. Most probably, the use of a fluorescent probe favoured the differentiation of such lipid domains in the above-mentioned techniques. The presence of the myriad of lipid structures led to slight topographic differences inappreciable by AFM.

The overall similar physical state and elasticity of all the studied PE:PG and PE:CL mixtures, points out that bacteria modify their lipid composition upon environmental changes to modify the membrane-protein interaction. The PE headgroup establishes strong intermolecular hydrogen bonds with neighbouring bilayer stabilizing phospholipids, forming an ion pair between the positively charged amine of one phospholipid and the negatively charged phosphate. (Yeagle, 2014) Therefore, it reduces the polar character of the membrane surface and facilitates the interaction with membrane proteins, being its extent dependent upon protein conformation, which may be influenced by the bindings of the phospholipids (Yeagle, 2014). In this line, it was demonstrated that the physiological activity of many transmembrane proteins is governed by their intermolecular hydrogen bonding with surrounding lipids containing PE headgroup. (Bazzi et al., 1992; Cronan, 2003) Romantsov et al. (Romantsov et al., 2009) demonstrated the influence of PG and CL on the functions of the osmosensor and osmoregulatory proteins in *E. coli*. Additionally, CL presents the possibility of resonance structures of its headgroup that can easily absorb or release a proton, which may play a role in membrane protein function. (Yeagle, 2014)

Therefore, it has been concluded that minor changes in membrane elasticity and physical state are achieved because of bacterial adaptation to external stimuli. Consequently, it is suggested that the changes in the lipid composition, e.g. lipid nature may regulate the activity of membrane proteins rather than modulate the physical properties of the membrane. The targettability of new antibacterial agents could be accordingly enhanced.

4. Conclusions

Biomimetic membranes composed of lipid mixtures (PE:PG and PE:CL) and the individual lipids extracted from *E.coli* were prepared using the Langmuir and LB techniques. PE:PG system showed ideal mixing behaviour and LE state at all the molar ratios studied, whereas PE:CL system presents the same physical state with non-ideal mixing behaviour. The PE:CL mixtures were non-favoured when the amount of PE or CL was between 20 and 50% and $\pi \geq 30\ mN{\cdot}m^{-1}$, in which the presence of domains was not observed by AFM. The presence of several

unsaturations in the lipids structures confers to the biomimetic membranes high elasticity that slightly vary as a function of the lipid composition. Therefore, bacteria adaptation to environmental signals by changing its lipid composition negligibly affect the rigidity of the bacterial inner membrane, suggesting that such changes might influence the membrane proteins activity.

Notes

The authors declare no competing financial interest.

Acknowledgements

This work was supported by the Spanish National Project HybridNanoCoat, “Hybrid nanocoatings on indwelling medical devices with enhanced antibacterial and antibiofilm efficiency” (MAT2015-67648-R).

References

Baumgärtner, P., Geiger, M., Zieseniss, S., Malleier, J., Huntington, J.A., Hochrainer, K., Bielek, E., Stoeckelhuber, M., Lauber, K., Scherfeld, D., Schwille, P., Wäldele, K., Beyer, K., Engelmann, B., 2007. Phosphatidylethanolamine critically supports internalization of cell-penetrating protein C inhibitor. J. Cell Biol. 179 (4), 793–804.

Bazzi, M.D., Youakim, M.A., Nelsestuen, G.L., 1992. Importance of phosphatidylethanolamine for association of protein kinase C and other cytoplasmic proteins with membranes. Biochemistry 31 (4), 1125–1134.

Benamara, H., Rihouey, C., Jouenne, T., Alexandre, S., 2011. Impact of the biofilm mode of growth on the inner membrane phospholipid composition and lipid domains in Pseudomonas aeruginosa. Biochim. Biophys. Acta Biomembr. 1808 (1), 98–105.

Bottier, C., Géan, J., Artzner, F., Desbat, B., Pézolet, M., Renault, A., Marion, D., Vié, V., 2007. Galactosyl headgroup interactions control the molecular packing of wheat lipids in langmuir films and in hydrated liquid-crystalline mesophases. Biochim. Biophys. Acta Biomembr. 1768 (6), 1526–1540.

Boyd, K.J., Alder, N.N., May, E.R., 2017. Buckling under pressure: curvature-based lipid segregation and stability modulation in cardiolipin-containing bilayers. Langmuir 33 (27), 6937–6946.

Castellana, E.T., Cremer, P.S., 2006. Solid supported lipid bilayers: from biophysical studies to sensor design. Surf. Sci. Rep. 61 (10), 429–444.

Cevc, G., Marsh, D., 1987. Phospholipid bilayers. In: Chapman, D. (Ed.), Physical Principles and Models.

Chen, Y., Sun, R., Wang, B., 2011. Monolayer behavior of binary systems of betulinic acid and cardiolipin: thermodynamic analyses of langmuir monolayers and afm study of langmuir-blodgett monolayers. J. Colloid Interface Sci. 353 (1), 294–300.

Clausell, A., Garcia-Subirats, M., Pujol, M., Busquets, M.A., Rabanal, F., Cajal, Y., 2007. Gram-negative outer and inner membrane models: insertion of cyclic cationic lipopeptides. J. Phys. Chem. B 111 (3), 551–563.

Cronan, J.E., 2003. Bacterial membrane lipids: where do we stand? Annu. Rev. Microbiol. 57 (1), 203–224.

de Mendoza, D., Cronan, J.E., 1983. Thermal regulation of membrane lipid fluidity in Bacteria. Trends Biochem. Sci. 8 (2), 49–52.

Dennison, S.R., Morton, L.H.G., Shorrocks, A.J., Harris, F., Phoenix, Da., 2009. A study on the interactions of aurein 2.5 with bacterial membranes. Colloids Surf. B Biointerfaces 68 (2), 225–230.

Dennison, S.R., Morton, L.H.G., Harris, F., Phoenix, D.A., 2014. The interaction of aurein 2.5 with fungal membranes. Eur. Biophys. J. 43 (6–7), 255–264.

Domènech, Ò., Morros, A., Cabañas, M.E., Montero, M.T., Hernández-Borrell, J., 2007. Thermal response of domains in cardiolipin content bilayers. Ultramicroscopy 107 (10–11), 943–947.

Dowhan, W., Bogdanov, M., 2012. Molecular genetic and biochemical approaches for defining lipid-dependent membrane protein folding. Biochim. Biophys. Acta Biomembr. 1818 (4), 1097–1107.

Fernandes, M.M., Ivanova, K., Hoyo, J., Pérez-Rafael, S., Francesko, A., Tzanov, T., 2017. Nanotransformation of vancomycin overcomes the intrinsic resistance of gram-negative bacteria. ACS Appl. Mater. Interfaces 9 (17), 15022–15030.

Ferreres, G., Bassegoda, A., Hoyo, J., Torrent-Burgués, J., Tzanov, T., 2018. Metal-enzyme nanoaggregates eradicate both gram positive and negative bacteria and their biofilms. Appl. Mater. Interfaces 10 (47), 40434–40442.

Gidalevitz, D., Ishitsuka, Y., Muresan, A.S., Konovalov, O., Waring, A.J., Lehrer, R.I., Lee, K.Y.C., 2003. Interaction of antimicrobial peptide protegrin with biomembranes. Proc. Natl. Acad. Sci. U. S. A. 100 (11), 6302–6307.

Horvath, S.E., Daum, G., 2013. Lipids of mitochondria. Prog. Lipid Res. 52 (4), 590–614.

Hoyo, J., Torrent-Burgués, J., Guaus, E., 2012. Biomimetic monolayer films of monogalactosyldiacylglycerol incorporating ubiquinone. J. Colloid Interface Sci. 384 (1), 189–197.

Hoyo, J., Guaus, E., Oncins, G., Torrent-Burgués, J., Sanz, F., 2013. Incorporation of Ubiquinone in supported lipid bilayers on ITO. J. Phys. Chem. B 117 (25), 7498–7506.

Hoyo, J., Guaus, E., Torrent-Burgués, J., Sanz, F., 2015a. Biomimetic monolayer films of digalactosyldiacylglycerol incorporating plastoquinone. Biochim. Biophys. Acta Biomembr. 1848 (6), 1341–1351.

Hoyo, J., Guaus, E., Torrent-Burgues, J., Sanz, F., 2015b. Electrochemistry of LB films of mixed MGDG:UQ on ITO. Bioelectrochemistry 104, 26–34. https://doi.org/10.1016/j.bioelechem.2015.02.006.

Hoyo, J., Guaus, E., Torrent-Burgués, J., 2016. Monogalactosyldiacylglycerol and digalactosyldiacylglycerol role, physical states, applications and biomimetic monolayer films. Eur. Phys. J. E 39 (3), 1–11.

Ivanova, K., Ramon, E., Hoyo, J., Tzanov, T., 2017. Innovative approaches for controlling clinically relevant biofilms. Curr. Trends Futur. Prospect. 17 (17), 1889–1914.

Ivanova, A., Ivanova, K., Hoyo, J., Heinze, T., Sanchez-Gomez, S., Tzanov, T., 2018. Layer-by-Layer decorated nanoparticles with tunable antibacterial and antibiofilm properties against both gram-positive and gram-negative bacteria. ACS Appl. Mater. Interfaces 10 (4), 3314–3323.

Khalifat, N., Fournier, J.B., Angelova, M.I., Puff, N., 2011. Lipid packing variations induced by PH in cardiolipin-containing bilayers: the driving force for the cristae-like shape instability. Biochim. Biophys. Acta Biomembr. 1808 (11), 2724–2733.

Kowal, J., Wu, D., Mikhalevich, V., Palivan, C.G., Meier, W., 2015. Hybrid polymer-lipid films as platforms for directed membrane protein insertion. Langmuir 31, 4868–4877.

Larsson, G., Törnkvist, M., 1996. Rapid sampling, cell inactivation and evaluation of low extracellular glucose concentrations during fed-batch cultivation. J. Biotechnol. 49 (1–3), 69–82.

Lee, A.G., 2003. Lipid-protein interactions in biological membranes: a structural perspective. Biochim. Biophys. Acta Biomembr. 1612 (1), 1–40.

Lee, A.G., 2004. How lipids affect the activities of integral membrane proteins. Biochim. Biophys. Acta Biomembr. 1666 (1–2), 62–87.

López-Montero, I., Arriaga, L.R., Monroy, F., Rivas, G., Tarazona, P., Vélez, M., 2008. High fluidity and soft elasticity of the inner membrane of Escherichia Coli revealed by the surface rheology of model langmuir monolayers. Langmuir 24 (8), 4065–4076.

López-Montero, I., Arriaga, L.R., Rivas, G., Vélez, M., Monroy, F., 2010. Lipid domains and mechanical plasticity of Escherichia coli lipid monolayers. Chem. Phys. Lipids 163 (1), 56–63.

Lupi, S., Perla, A., Maselli, P., Bordi, F., Sennato, S., 2008. Infrared spectra of phosphatidylethanolamine-Cardiolipin binary system. Colloids Surf. B Biointerfaces 64 (1), 56–64.

Michel, J.P., Wang, Y.X., Dé, E., Fontaine, P., Goldmann, M., Rosilio, V., 2015. Charge and aggregation pattern govern the interaction of Plasticins with LPS monolayers mimicking the external leaflet of the outer membrane of gram-negative bacteria. Biochim. Biophys. Acta Biomembr. 1848 (11), 2967–2979.

Michel, J.P., Wang, Y.X., Kiesel, I., Gerelli, Y., Rosilio, V., 2017. Disruption of asymmetric lipid bilayer models mimicking the outer membrane of gram-negative bacteria by an active Plasticin. Langmuir 33 (41), 11028–11039.

Murzyn, K., Róg, T., Pasenkiewicz-Gierula, M., 2005. Phosphatidylethanolamine-phosphatidylglycerol bilayer as a model of the inner bacterial membrane. Biophys. J. 88 (2), 1091–1103.

Popova, A.V., Hincha, D.K., 2003. Intermolecular interactions in dry and rehydrated pure and mixed bilayers of phosphatidylcholine and digalactosyldiacylglycerol: a fourier transform infrared spectroscopy study. Biophys. J. 85 (3), 1682–1690.

Purrucker, O., Förtig, A., Jordan, R., Tanaka, M., 2004. Supported membranes with well-defined polymer tethers - incorporation of cell receptors. ChemPhysChem 5 (3), 327–335.

Roche, Y., Peretti, P., Bernard, S., 2006. Influence of the chain length of ubiquinones on their interaction with DPPC in mixed monolayers. Biochim. Biophys. Acta Biomembr. 1758 (4), 468–478.

Róg, T., Hector, M.S., Munck, N., Oresic, M., Karttunen, M., Vattulainen, I., 2009. Role of Cardiolipins in the inner mitochondrial membrane: insight gained through atom-scale simulations. J. Phys. Chem. B 113 (11), 3413–3422.

Romantsov, T., Guan, Z., Wood, J.M., 2009. Cardiolipin and the osmotic stress responses of bacteria. Biochim. Biophys. Acta Biomembr. 1788 (10), 2092–2100.

Salat, M., Petkova, P., Hoyo, J., Perelshtein, I., Gedanken, A., Tzanov, T., 2018. Durable antimicrobial cotton textiles coated sonochemically with ZnO nanoparticles embedded in an in-situ enzymatically generated bioadhesive. Carbohydr. Polym. 189 (February), 198–203.

Sanchez, J., Badia, A., 2003. Atomic force microscopy studies of lateral phase separation in mixed monolayers of Dipalmitoylphosphatidylcholine and dilauroylphosphatidylcholine. Thin Solid Films 440 (1), 223–239.

Schlame, M., Rua, D., Greenberg, M.L., 2000. The biosynthesis and functional role of cardiolipin. Prog. Lipid Res. 39 (3), 257–288.

Shokri, A., Larsson, G., 2004. Characterisation of the Escherichia coli membrane structure and function during fedbatch cultivation. Microb. Cell Fact. 3, 9.

Vance, J.E., 2015. Phospholipid synthesis and transport in mammalian cells. Traffic 16 (1), 1–18.

Vitovič, P., Nikolelis, D.P., Hianik, T., 2006. Study of Calix[4]Resorcinarene-Dopamine complexation in mixed phospholipid monolayers formed at the air-water interface. Biochim. Biophys. Acta Biomembr. 1758 (11), 1852–1861.

Wydro, P., Flasiński, M., Broniatowski, M., 2012. Molecular organization of bacterial membrane lipids in mixed systems—a comprehensive monolayer study combined with grazing incidence X-Ray diffraction and brewster angle microscopy experiments. Biochim. Biophys. Acta Biomembr. 1818 (7), 1745–1754.

Yeagle, P.L., 2014. Non-covalent binding of membrane lipids to membrane proteins. Biochim. Biophys. Acta Biomembr. 1838 (6), 1548–1559.

Yeagle, P.L., 2016. The Membranes of Cells. Academic Press-Elsevier, San Diego, California.